Numerical Modeling of Internal Heating Curing of Glass Reinforced Epoxy Pipes

Hugo A. Flores,[1] **Laura Alejandra Fasce,**[2] **Carmen C. Riccardi,**[2] **María Alejandra Ayude**[2]
[1] *Laboratorio Tubhier S.A., Villa Mercedes, Argentina*
[2] *INTEMA-CONICET-UNMdP, J.B. Justo 4302, (B7608FDQ) Mar del Plata, Argentina*

A dynamic one-dimensional model is developed to simulate the novel internal heating curing process in the manufacturing of glass reinforced epoxy pipes by filament winding. The model combines the energy balance with a mechanistic kinetic approach and it is experimentally validated using industrial plant data. The efficiency of a specific curing cycle at different operating conditions is analyzed. In particular, the influence of ambient temperature, initial mandrel temperature, glass fiber content, initiator concentration and pipe wall thickness on temperature, and degree of cure profiles within the pipe wall thickness is discussed. This study attempts to dispel current industrial myths and to propose practical strategies to improve the internal heating curing process. POLYM. ENG. SCI., 55:2626–2635, 2015. © 2015 Society of Plastics Engineers

INTRODUCTION

The Filament Winding process is a manufacturing method widely used to produce high quality pipes made of fiber reinforced thermosetting composites. Typically, fibers are impregnated in a resin bath and wounded around a rotating mandrel. Afterward, the assembly is heated to induce matrix curing, that is, resin polymerization.

A proper curing strategy is essential to obtain homogeneous matrix curing and to avoid pipe defects such as residual stresses and strains or entrapped gas bubbles. The generation of smooth temperature and conversion profiles within the pipe wall thickness is fundamental to ensure high quality products [1, 2]. Residual strains are generated by thermal expansion and contraction of the composite and by chemical shrinkage of the matrix. These strains are found to be proportional to the temperature and conversion degree gradients developed during curing, respectively [3].

Traditionally, curing is carried out by external heating methods, for example, in ovens under air or inert atmospheres, in gas-fired ovens, in microwave ovens, or in autoclaves [4–6]. In these methods, matrix gelation occurs from the outside to the inside of the pipe. Alternatively, internal heating methods have been recently proposed. For example, Xu et al. [7] introduced the use of flowing steam inside the mandrel to produce curing. In these methods, matrix conversion progresses from the inside to the outside of the pipe. Lee et al. [8] found that internal heating leads to a more uniform temperature distribution than external heating resulting in a final product with lower residual stresses. Therefore, internal heating curing appears to be a very convenient alternative to traditional methods in the filament winding process.

Numerical modeling of the curing process is an effective way of analyzing the influence of operating variables on the temperature and curing degree distributions and hence on the quality of final pipes. The development of an adequate model allows reducing project times and avoids costly trial-and- error experiences in the pipe manufacturing industry.

Most of the published works dealing with modeling of curing process in filament winding focuses on external heating [1, 9, 10], whereas only a few contributions copes with internal heating [7, 11].

Generally, in numerical models the polymerization reaction rate is described using phenomenological or empirical kinetic approaches [1, 2, 7, 11–13]. Kinetic parameters are determined for specific temperature conditions and reactive systems that are usually commercial and of unknown composition. Therefore, the prediction capability of those kinetic models is confined to particular conditions, and the curing model results in a rather limited analysis tool.

In this work, a simple mathematical model is developed to simulate the internal heating curing of glass reinforced epoxy (GRE) pipes manufactured by filament winding in an existent industrial process. A dynamic one-dimensional model is proposed and solved by an explicit finite differences scheme. The geometrical simplification of the problem is reasonable since the pipe is considered as a long hollow cylinder that is uniformly heated from the inside and exposed to homogeneous ambient conditions [1]. Transient temperature gradient is assumed to occur only in the radial direction and edge effects are neglected.

The reactive system is composed of an epoxy/anhydride mixture with a quaternary amine used as initiator, which is one of the most commonly used formulations for GRE pipes production. The curing process of GRE pipes involves heat conduction and exothermic polymerization reaction between the epoxy and anhydride groups. A novelty in the proposed model is the inclusion of a mechanistic kinetic approach to depict the reaction rate. The kinetic model has been first proposed and validated for the copolymerization of other epoxy-anhydride system initiated by a ternary amine [14, 15]. It has been recently calibrated for the industrial reactive mixture used here in a wide range of temperature conditions, initiator concentrations and glass fiber (GF) contents [16]. The incorporation of a mechanistic instead of an empirical kinetic approach enhances the prediction capability of the curing process model.

The dynamic one-dimensional model is cross-validated using industrial plant data. The experimental validation together with the inclusion of a mechanistic kinetic approach allows the development a powerful tool for the design and analysis of internal heating curing cycles.

Correspondence to: M.A. Ayude; e-mail: mayude@fi.mdp.edu.ar
DOI 10.1002/pen.24155
Published online in Wiley Online Library (wileyonlinelibrary.com).

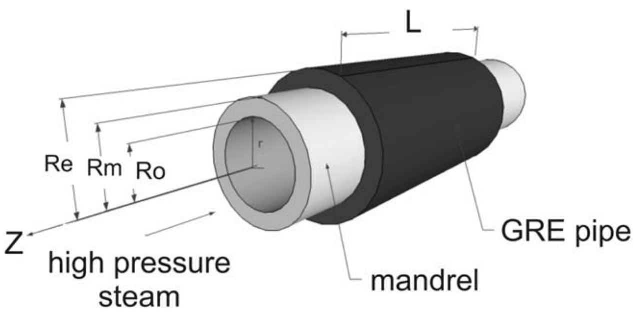

FIG. 1. Geometrical representation of the mandrel/glass reinforced epoxy composite pipe system.

TABLE 1. Parameters values used in the numerical model.

Parameter		Value (units)
Glass fibers	ρ_g	2540 (kg/m^3)
	C_{Pg}	0.199 kcal/(kg°C)
Resin	ρ_r	1220 (kg/m^3)
Glass reinforced epoxy composite	ρ_c	$v_g.\ \rho_g + v_r.\ \rho_r$
	C_{Pc}	$v_r.\ (1.96 + 2.5 \times 10^{-3}.\ T - 0.59\ .\alpha) + v_g.\ C_{Pg}{}^a$ [kcal/(kg°C)]
H		0.24 kcal/(min m^2 °C)
k_C		0.0044 kcal/(min m °C)

$^a v = \%$wt.

In this article, the model is used to analyze the efficiency of a specific curing cycle under different operation conditions. The effects of key processing variables—ambient temperature, initial mandrel temperature, GF content, initiator concentration and pipe wall thickness—on the temporal development of the radial temperature, conversion, and glass transition temperature (T_g) profiles are evaluated. An attempt is made to dispel current industrial myths.

EXPERIMENTAL

Filament Winding Process

A brief description of the industrial process simulated in this article is presented in this section.

GRE pipes are produced by filament winding in a manufacturing plant located in Villa Mercedes, San Luis, Argentina. Composite pipes of different nominal internal diameters (2, 3, and 6 inches) containing about 73 %wt of alkali free alumino-borosilicate GFs (E-type) are produced. The matrix reactive system is a stoichiometric mixture of diglycidyl ether of bisphenol A (DGEBA) and methyltetrahydroftalic anhydride (MTHPA) with a quaternary amine, benzyltriethylammonium chloride (BTEAC), added as initiator. Different BTEAC concentrations in MTHPA are used (3, 4, 5.5 %wt).

GFs are impregnated in a resin bath and wrapped around the rotating steel mandrel (mold). Matrix curing by internal heating is carried out after the winding process. High pressure steam enters into the mandrel and imposes the temperature evolution according to the desired curing cycle. The mandrel design ensures a homogeneous temperature distribution on the surface that is in contact with the pipe inner face; no water condensation occurs. The curing process is carried out under forced air circulation ambient conditions, which provides a uniform temperature in the surrounds of the pipe outer face.

Industrial Plant Measurements

Industrial plant measurements are carried out to validate the mathematical model as described later in "Estimation of Model Parameters." A specially-designed device is used to register the temporal evolution of the temperature in the internal and external pipe wall faces. Type K thermocouples are located in the steel/GRE composite surface and in the GRE composite/air surface. Thermocouples' signals are acquired every 3 s.

Measurements are performed at the same ambient and mandrel initial temperatures (35°C) for three processing conditions:

a. 3″ internal diameter, 5.6 mm wall thickness, 73.5 %wt. GF, and 3 %wt. BTEAC in MTHPA.

b. 2″ internal diameter, 4.5 mm wall thickness, 73.5 %wt. GF, and 3 %wt. BTEAC in MTHPA.

c. 6″ internal diameter, 10 mm wall thickness, 73.5 %wt. GF, and 4 %wt. BTEAC in MTHPA.

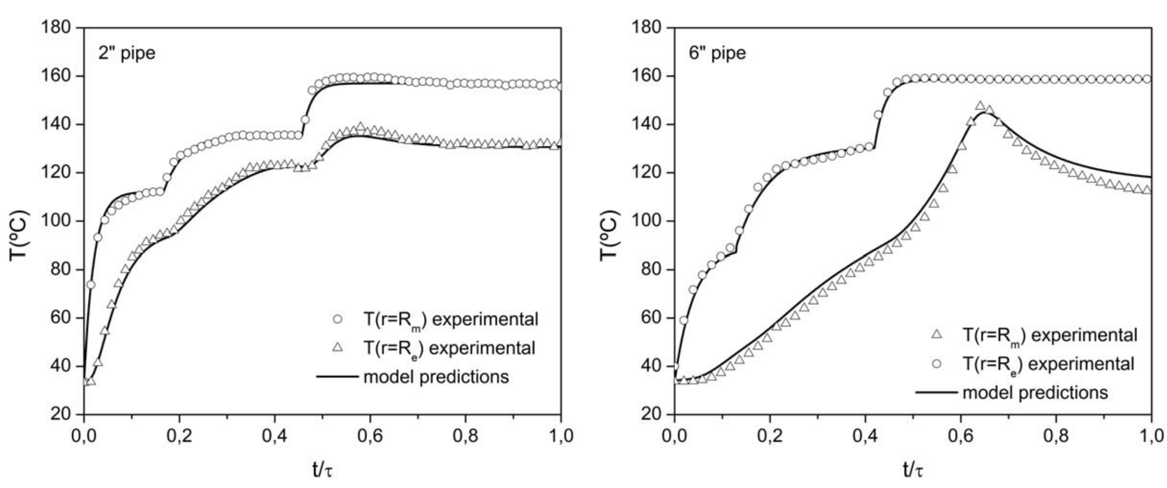

FIG. 2. Experimental and predicted temperature-time profiles at the inner and outer faces of GRE pipes used for model validation. Conditions corresponds to cases b and c given in "Industrial Plant Measurements."

TABLE 2. Processing parameters defined in the case studies (fixed values or variation range). Simulations carried out for a 3″ internal diameter pipe with the curing cycle given by *Eq. 8*.

Processing parameter	Case study				
	No. 1	No. 2	No. 3	No. 4	No. 5
Ambient temperature, T_a (°C)	**–20–40**	35	35	35	35
Initial mandrel temperature, T_0 (°C)	35	**35–110**	40	40	40
Glass Fiber content (% wt GF)	73	73	**70–80**	73	73
Initiator concentration (BTEAC %wt in MTHPA)	3	3	3	**3, 4, 5.5**	3
Wall thickness (mm)	5.6	5.6	5.6	5.6	**3–15**

NUMERICAL MODEL

Kinetic Model

A mechanistic kinetic model is adopted to describe the reaction rate of the industrial DGEBA/MTHPA/BTEAC reactive system [13]. The reaction mechanism includes an activation reversible step that transforms inactive specie (I) into active one (I^*), followed by a propagation step, in which the addition of an epoxy/anhydride couple (M) to the growing chain takes place. Thus, the mechanism of reaction and the kinetic equations are:

Activation step: $I \underset{k_1}{\overset{k_1}{\rightleftarrows}} I^*$

$$\frac{dI}{dt} = k_1 I_0 - (k_1 - k_{-1}) I* \tag{1}$$

Propagation step: $I^* + M \xrightarrow{h_p} I^*$

$$\frac{d\alpha}{dt} = k_p I * (1-\alpha) \tag{2}$$

where α is the epoxy (or anhydride) group conversion, I_0 is the initial concentration of the quaternary amine and k_1, k_{-1}, and k_p are the kinetic constants with an Arrhenius-type temperature dependence.

The activation step is assumed to be independent on initiator concentration while the propagation step depends on it. The presence of GFs does not influence the kinetic mechanism [16]. The kinetic model parameters are taken from Flores et al. [16].

Internal Heating Curing Model

Figure 1 shows the geometrical representation of the system once the winding stage is completed. The macroscopic behavior of the curing process can be simply depicted by an energy balance. Under the following assumptions:

a. the geometry of GRE pipes can be considered as an infinite hollow cylinder; implying radial thermal flow and negligible axial and angular dispersions,
b. homogeneous temperature distribution inside the mandrel,
c. flat temperature profile along the steel mandrel thickness,

the energy balance accounting for the heat generated by the copolymerization reaction can be written as:

$$\rho_C . C_{PC} . \frac{\partial T}{\partial t} = k_C \left[\frac{\partial^2 T}{\partial r^2} + \frac{1}{r}\frac{\partial T}{\partial r} \right] + w_r . \rho_r . (-\Delta H) \cdot \frac{d\alpha}{dt} \tag{3}$$

where T is the absolute temperature, r is the radial coordinate, t is the time, ρ_C and ρ_r are the density values of the glass reinforce epoxy composite and the resin, respectively, C_{PC} is the

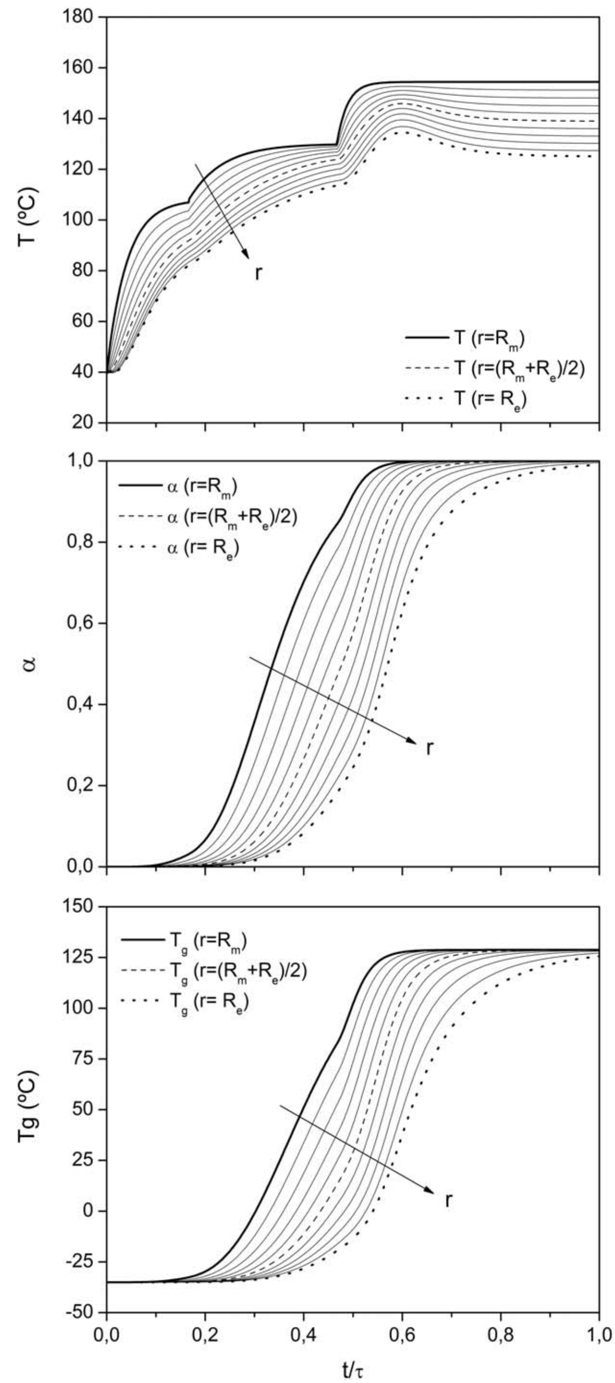

FIG. 3. Temporal evolution of temperature, conversion and T_g at different radial positions within the pipe wall during curing. Simulation conditions correspond to the base case detailed in "Case Studies."

 DOI 10.1002/pen

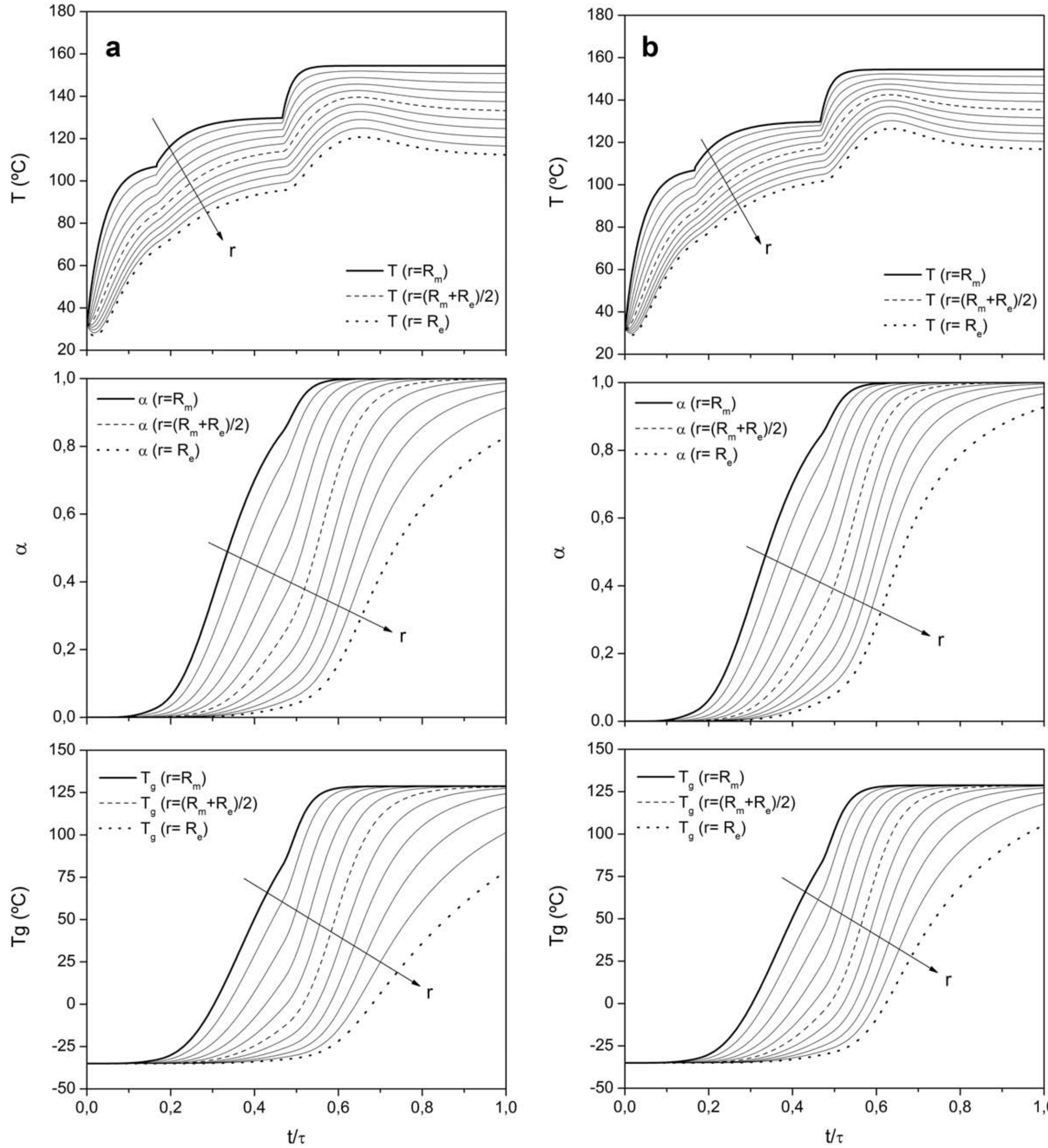

FIG. 4. Temporal evolution of temperature, conversion and T_g at different radial positions for various ambient temperatures: (a) –20, (b) 0, (c) 20, and (d) 40 °C. Simulation conditions: case no. 1 (Table 2).

heat capacity value of the GRE composite, k_C is the thermal conductivity, w_r is the resin mass, and ΔH is the total heat of reaction.

The following initial and boundary conditions are considered:

$$t=0 \quad \forall r \quad T=T_0 \quad \alpha=0 \quad I^*=0 \tag{4}$$

$$r=R_m \quad \forall t \quad T=T_s(t) \tag{5}$$

$$r=R_e \quad \forall t \ \frac{\partial T}{\partial r}=\frac{h_{eff}}{k_c}(T_a-T) \tag{6}$$

where T_0 is the mandrel temperature, T_s is the steam temperature, h_{eff} is the effective heat transfer coefficient, and T_a is the ambient temperature.

The resolution of *Eqs. 1–3* gives the temporal evolution of the radial temperature and conversion profiles.

Due to the proprietary and confidential nature of company data, model and experimental outcomes are reported in terms of a dimensionless time (t^*), which was calculated normalizing the time, t, by the whole curing cycle duration, τ.

The model also includes the estimation of the matrix glass transition temperature, T_g, by means of the Di Benedetto equation [17]:

$$\frac{T_g-T_{g0}}{T_{g\infty}-T_{g0}}=\frac{\lambda\alpha}{1-(1-\lambda)\alpha} \tag{7}$$

where T_{g0} is the glass transition temperature of the un-reacted system, $T_{g\infty}$ the glass transition temperature of the completely cured system, and λ the ratio between the corresponding changes of heat capacities. Values of –35.6, 128.7, and 0.47°C for T_{g0}, $T_{g\infty}$, and λ respectively, are taken from a previous work [16].

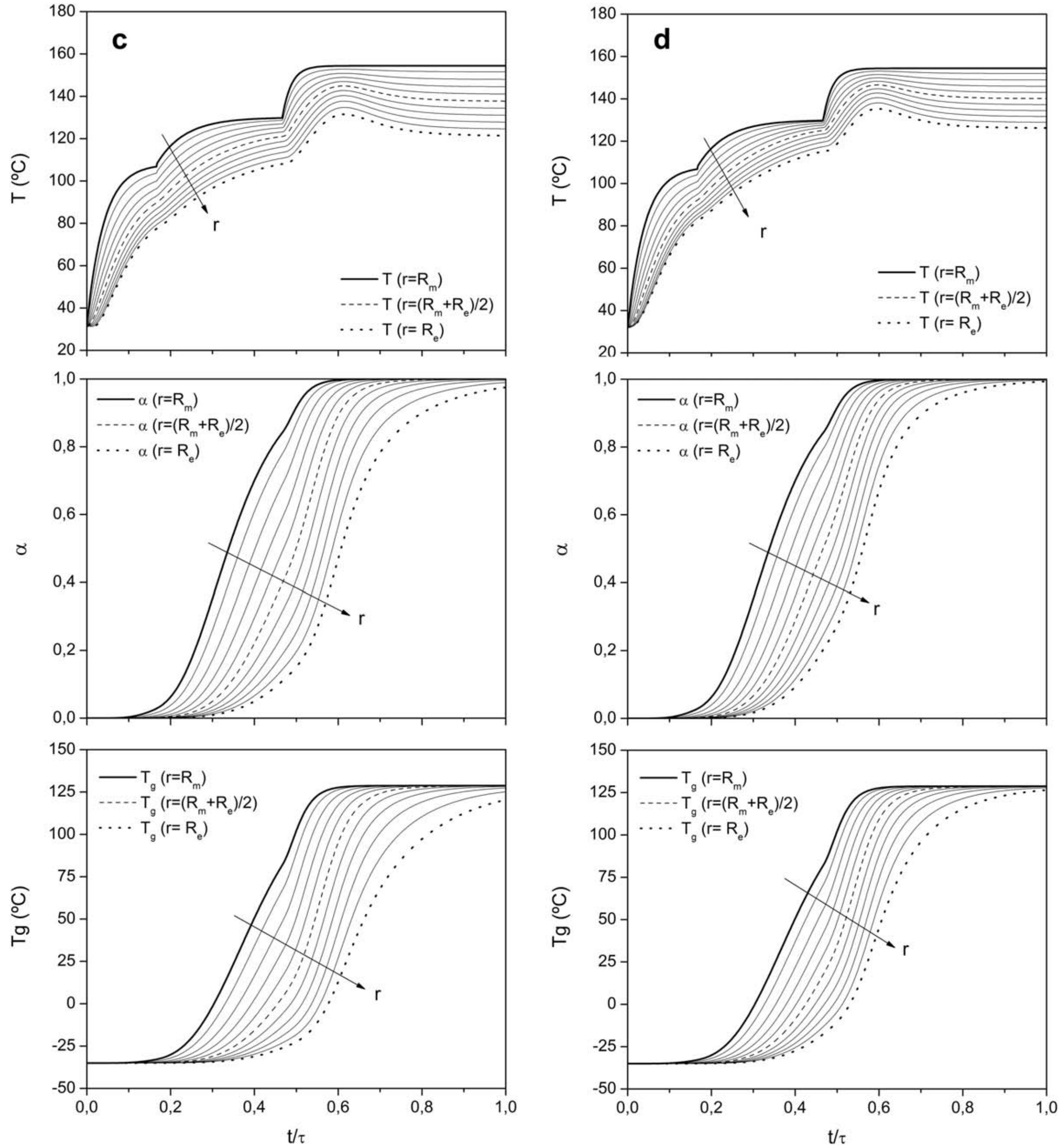

FIG. 4. (*Continued*)

Estimation of Model Parameters

The curing cycle is imposed by the temperature of the steam that flows inside the mandrel, T_s(t). A three-step curing cycle, currently used in the pipe production process, is adopted in numerical simulations. The curing cycle is introduced into the model as the boundary condition for the pipe inner face (see *Eq.* 5). To define $T_s(t)$, steam temperature data are experimentally obtained and fitted by Least Squares to a three-part function. Each part has the following mathematical form:

$$\mathrm{T_s} = a + b \cdot \exp\left(\frac{-\frac{t}{\tau}}{c}\right) \tag{8}$$

where the temperature is expressed in °C. The fitted coefficients of *Eq. 8* are: $a = 105$, $b = -76.2$, and $c = 0.029$ for $0 \leq t/\tau < 0.15$; $a = 130$, $b = -213.8$, and $c = 0.069$ for $0.15 \leq t/\tau < 0.46$; and $a = 154$, $b = -4 \times 10^{10}$, and $c = 0.022$ for $0.46 \leq t/\tau \leq 1$. In all cases, R^2 is larger than 0.98.

Numerical model parameters are summarized in Table 1. The properties of GFs are directly obtained from PPG Industries data sheet; the resin density is experimentally measured; and the GRE composite properties are evaluated according to Santiago et al. [18]. The total heat of reaction, ΔH, is taken as 49.3, 54.4, and 58.6 kJ/eq for systems containing 3, 4, and 5.5 %wt BTEAC in MTHPA, respectively [16].

Thermal conductivity and effective convective heat transfer coefficient are taken as model calibration parameters due to the difficulty in estimating their actual values in the industrial curing process. These parameters are assumed to be constant. The assumption for k_C is supported by its weakly dependency on temperature and degree of cure, as it was demonstrated for similar reactive systems [19]. The convective heat transfer is taken

 DOI 10.1002/pen

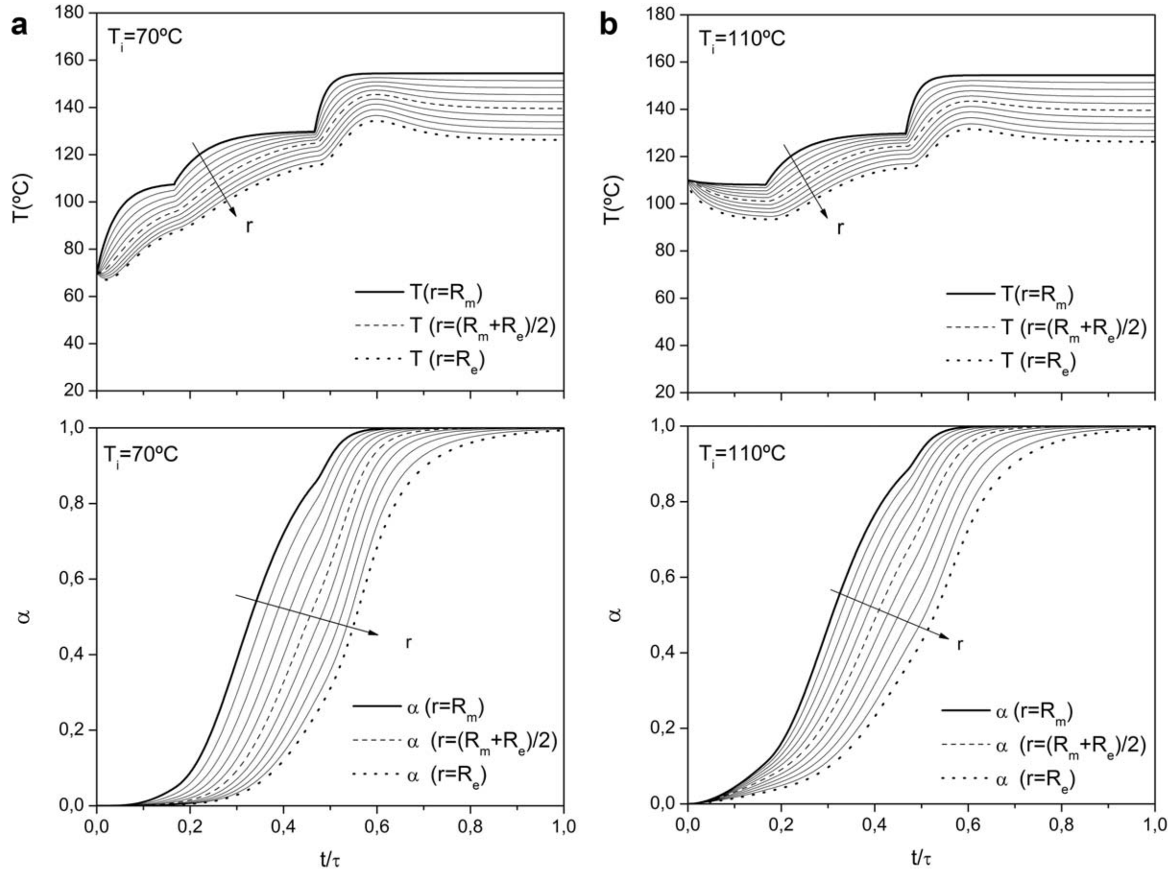

FIG. 5. Temporal evolution of temperature and conversion at different radial positions for various mandrel initial temperatures: (a) 70 °C, (b) 110 °C. Simulation conditions: case no. 2 (Table 2).

as an effective coefficient (h_{eff}) that takes into account the turbulent air flow conditions and the temperature evolution gradient between the air and the pipe surface.

k_C and h_{eff} parameters values given in Table 1 are obtained by fitting the experimental temperature-time measurements in the inner and the outer faces of the pipe for the condition *a* described in "Industrial Plant Measurements." For these values, the error between experimental and predicted profiles is lower than 4.2%. The fitted k_C and h_{eff} values are in agreement with those reported for similar systems [1, 8, 11].

Numerical Resolution

Differential *Eqs. 1–3* together with initial and boundary conditions (4–6) are re-written in terms of convenient dimensionless variables. The dimensionless system is numerically solved by an explicit finite difference scheme using forward difference approximation for the time derivative, central symmetric difference for the second-order space derivative and central difference for the first-order space derivative. The resolution is implemented in MathLab®. Time and space steps are initially set to satisfy the stability criteria for explicit finite difference scheme [20]. Once convergence is achieved, the accuracy of the solution is checked by further reducing the steps.

Model Validation

The internal heating curing model is cross-validated using two independent sets of temperature-time profiles in the inner and the outer faces of the pipe, that is, using datasets different from those considered for fitting h_{eff} and k_c. These sets correspond to conditions b and c depicted in section "Industrial plant measurements," and represent the minimum and maximum pipe internal diameters manufactured in the industrial plant. The excellent agreement found between measured and predicted temperature-time profiles is shown in Fig. 2. Thus, the model is assumed to be valid and adequate to describe the curing behavior of the GRE pipes reactive systems in a wide range of operating conditions.

Case Studies

The model is used as a process analysis tool to evaluate the influence of ambient temperature, initial mandrel temperature, GF content, initiator concentration, and pipe wall thickness on the temporal evolution of the radial temperature, conversion and T_g profiles.

The base case corresponds to the curing of a 3″ internal diameter pipe, 5.6 mm wall thickness, 73% wt. GF, 3 %wt. BTEAC in MTHPA at $T_a = 35°C$ and $T_0 = 40°C$. Simulations are carried out under the different scenarios described in Table 2. In all cases, the curing cycle is given by *Eq*. 8. It is known from experience in the manufacturing plant that, for the processing conditions of the base case, this curing cycle is optimal for material compacting, gas bubble excretion, and residual stresses minimization.

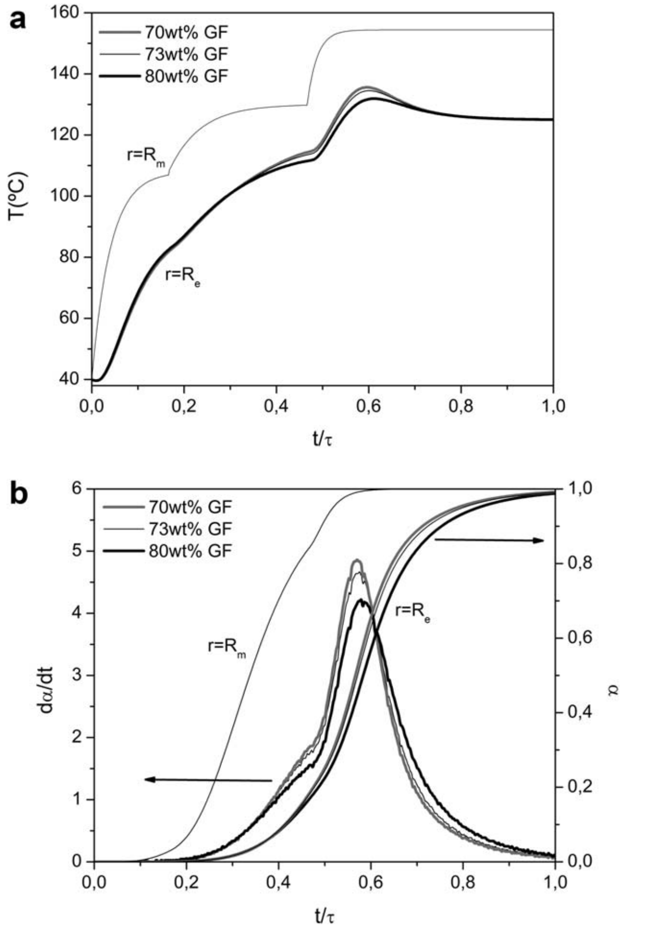

FIG. 6. Temporal evolution of temperature (a) and conversion and curing rate (b) predicted at the inner and outer faces of pipes with different glass fiber contents. Simulation conditions: case no. 3 (Table 2).

RESULTS AND DISCUSSION

Predicted temperature, conversion, and T_g profiles as a function of dimensionless time at different radial positions are shown in Fig. 3 for the base case conditions (Case Studies).

At any time of curing, temperature decreases from the inner to the outer faces of the pipe. Uniform temperature profiles are developed during the whole curing process. A smooth maximum in the temperature–time profiles is predicted within the third step of the curing cycle. This maximum becomes negligible toward the inner surface of the pipe. The temperature peak coincides with the maximum curing rate (dα/dt) in the outer surface.

The conversion gradually increases from the inside out layer by layer. The gelation conversion of the industrial reactive system is 0.52 [13]. Matrix gelation is achieved in the pipe inner face within the second step of the cycle, whereas in the outer face it is reached at approximately the time in which the temperature profile shows its maximum.

The T_g of the composite is progressively enlarged and the pipe body reaches the design value (125°C) at the end of the curing cycle.

In the following sections the effect of key processing variables on the temporal evolution of the radial temperature, conversion, and T_g profiles is presented.

Effect of Ambient Temperature

The manufacturing plant is situated in a geographical zone wherein the daily and seasonal thermal amplitudes are large. Ambient temperature reaches 40°C in summer and −20°C in winter and show daily variations of about 30°C in autumn and spring [21]. The industrial experience indicates that quality of the pipes is greatly affected by these drastic changes in the ambient conditions.

Figure 4 shows the temporal evolution of temperature, conversion and T_g profiles at different radial positions for four different ambient temperature conditions. Simulation conditions are given in case no. 1 (Table 2). In agreement with experience, the model predicts that radial temperature and conversion profiles are very sensitive to ambient temperature. The radial temperature gradients increase with decreasing ambient temperature and the radial conversion profiles follow the same trend. This implies that at low ambient temperatures, a wide distribution of matrix curing degree is developed within the pipe wall.

The analysis of conversion profiles reveals the existence of a critical ambient temperature. For case no. 1 conditions, this critical temperature appears to be around 20°C (Fig. 4c). Below this temperature, the outer layers of the pipe wall are not completely cured during the imposed cycle (Fig. 4a and b). Even though the matrix gelation conversion is achieved, the composite is far from its designed T_g. Above the critical temperature, the time needed to complete the curing is reduced as ambient temperature increases (Fig. 4d).

Simulation results demonstrate that ambient temperature constitutes a key processing parameter in the internal heating curing of GRE pipes. The curing cycle has to be tuned according to ambient temperature conditions in order to yield high-quality pipes.

Influence of Initial Mandrel Temperature

It is frequently believed in industry that, for a specific curing cycle, an increase in the initial mandrel temperature shortens production times. Simulations are performed at initial mandrel temperatures above the value set in the base case, as indicated in case no. 2 (Table 2). In simulations, it is assumed that during winding, the reactive mixture remains in contact with the mandrel enough time to reach the mold temperature (T_0). This assumption is not so far from reality.

Figure 5a and b compare the temporal evolution of temperature and conversion at different radial positions predicted for two initial mandrel temperatures (T_0) above 35°C. Temperature profiles are influenced by initial mandrel temperature only during the first step of the cycle. The higher the initial mandrel temperature is set, the higher is its influence on the temperature profiles. However, in this part of the cycle, matrix conversion is negligible. Therefore, contrary to what is believed, an increase in the initial mandrel temperature hardly contributes to reduce the time to achieve complete conversion in the GRE pipe body.

Influence of Fiber Content

The dispersion in the GF content in GRE pipes is inherent to the variability of the commercial GF fabricates. For example, the historic value of GF content in the industrial plant is about 75 ± 2 %wt [21]. The effect of GF content on the curing process is investigated in this section. Simulations are performed under

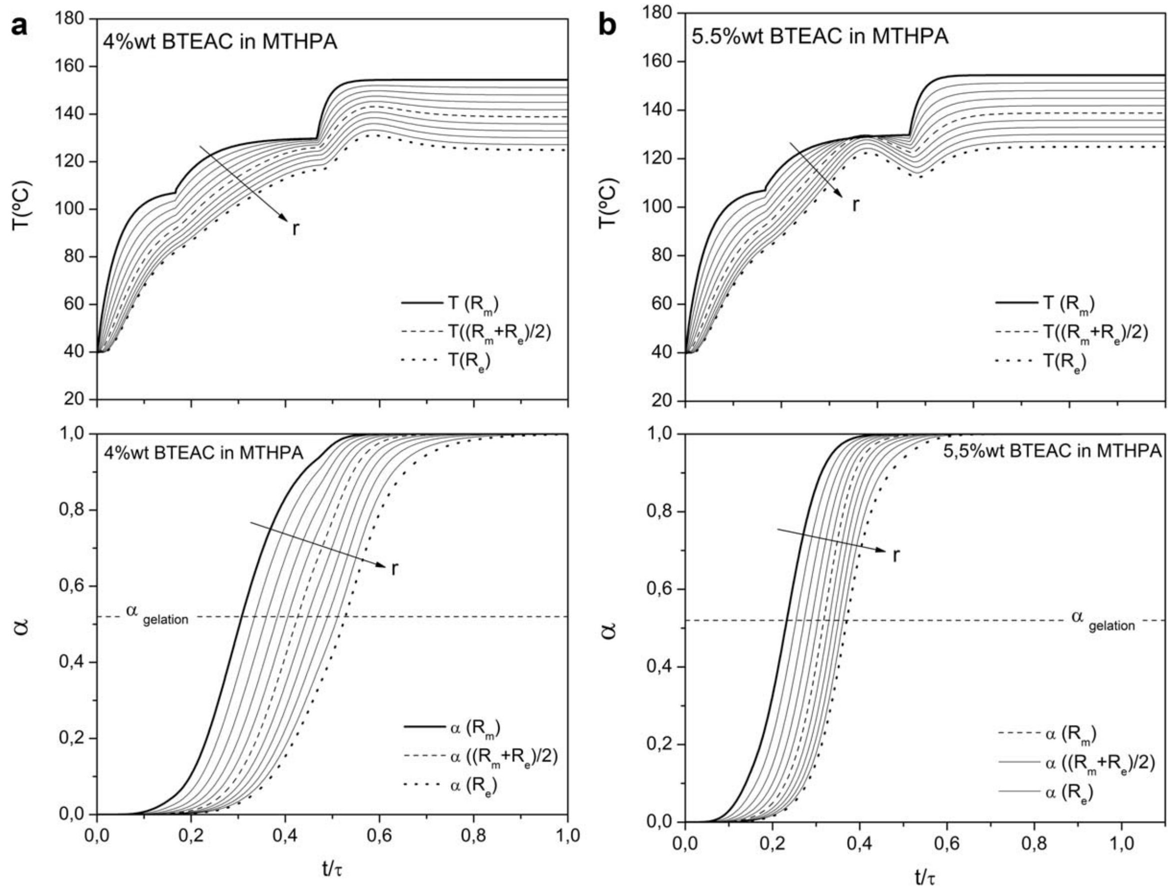

FIG. 7. Temporal evolution of temperature and conversion at different radial positions for two initiator concentrations: (a) 4 %wt BTEAC in MTHPA and (b) 5.5 %wt BTEAC in MTHPA. Curing rate-time profiles (c) predicted for different initiator concentrations. Simulation conditions: case no. 4 (Table 2).

the conditions given in case no. 3 (Table 2). Reinforcement content is varied between two limited values (70 and 80 %wt GF).

Predicted temperature–time profiles at the inner and the outer surfaces are shown in Figure 6a for three different GF contents. Only slight changes in the temperature profiles are predicted and confined to the near outer layers. The peak temperature increases and shifts to lower time as the GF content decreases.

Figure 6b compares the temporal evolution of conversion and curing rate in the outer surface. Under the imposed curing cycle, the pipe is completely cured independently of the GF content but the conversion history is different. The maximum in polymerization rate increases with decreasing GF content, leading to larger conversion and temperature gradients along time.

The generation of large gradients is accompanied with large residual strains in the pipe due to chemical shrinkage of the resin and thermal expansion and contraction of the composite [3, 11]. Therefore, the reduction is GF content detriments the pipe quality.

The predicted slight variations in temperature and conversion distributions with GF content may be explained considering two opposites phenomena. As the GF content decreases, the composite heat capacity increases (Table 1), inducing a decrease in temperature profile. At the same time, the heat generation rate increases, leading to a temperature rise. For the analyzed cases, both phenomena are globally compensated. As shown in Fig. 6a, after maximum conversion rates occur, the temperature profiles match each other, allowing complete curing even for the highest GF content (80 %wt GF).

The results presented here highlight that the actual variability of GF content has a slight effect on the curing behavior of the pipes. As a practical advice, the curing cycle should be optimized for the lowest fiber content.

Influence of Initiator Concentration

The effect of the BTEAC concentration on the pipe curing process is investigated in this section. Simulations are carried out for the conditions listed in Case no. 4 (Table 2). The mechanistic kinetic approach adopted in the model enables this analysis. A higher BTEAC concentration accelerates the propagation step of the polymerization reaction (*Eq. 2*).

Figure 7a and b presents the temporal evolution of temperature and conversion profiles at different radial positions for two initiator concentrations higher than the one considered in the base case (4 and 5.5 %wt BTEAC in MTHPA). Figure 7c compares the reaction rate profiles developed at the inner, middle, and outer layers.

As expected, the time needed to attain complete curing of the pipe is reduced when the BTEAC concentration is increased. An increase in the initiator concentration from 3 to 4 %wt, slightly reduce the curing time and smooth temperature and conversion profiles are predicted (see Figs. 3 and 7a. The shape of

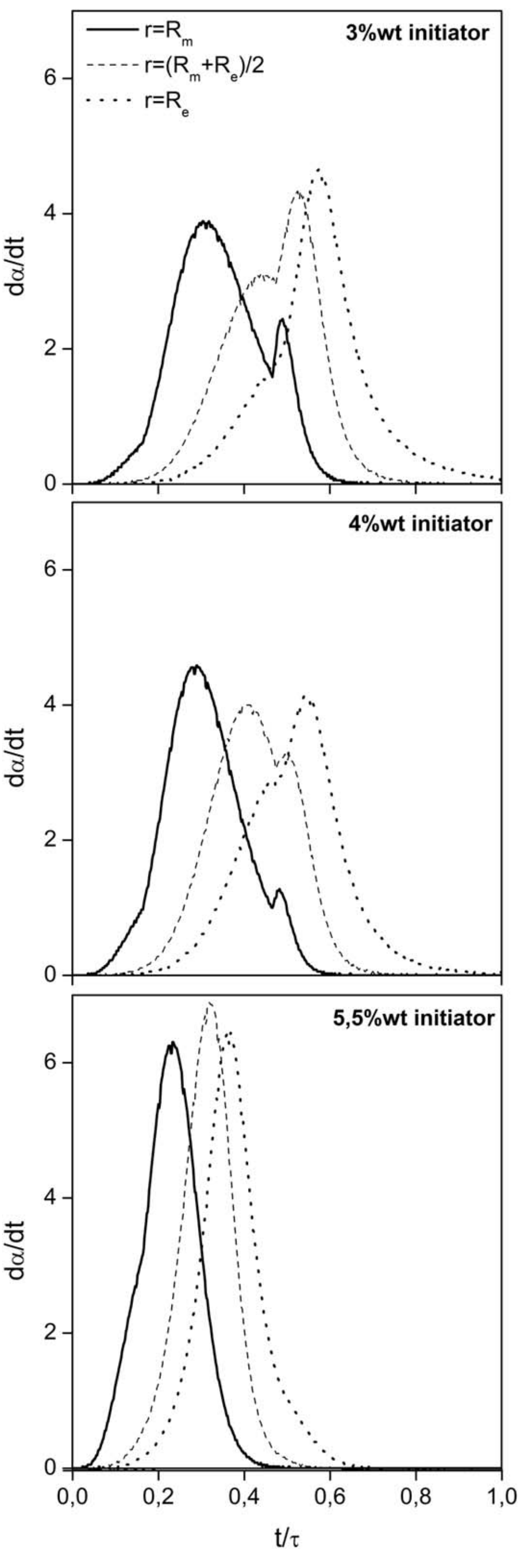

FIG. 7. (Continued).

the reaction rates profiles is altered but the maximum rate value is not significantly increased (Fig. 7c). On the contrary, for the highest BTEAC concentration, the temperature peak shifts to the second step of the cycle and significantly increases in magnitude (Fig. 7b). The maximum reaction rates are relatively high, inducing matrix gelation at earlier times and an abrupt curing process. This curing history is detrimental for the pipe quality, since the development of large residual strains is promoted and entrapped gas bubbles scape is prevented.

Influence of Pipe Wall Thickness

The pipe wall thickness for a specific nominal internal diameter is varied according to service pressure requirements. In practice, it is believed that the use of a curing cycle that results optimal for a given wall thickness may not be adequate for pipes with large thicknesses. To investigate this issue, simulations are carried out under the conditions stated in Case no. 5 (Table 2).

The temporal evolutions of temperature and conversion developed at the outer surface for pipes of different wall thickness (3 to 15 mm) are shown in Fig. 8a and b, respectively. An increase in the pipe wall thickness reduces the temperature level achieved during the curing process and increases the curing time. For a 3 mm wall thickness, the curing process proceeds with the development of smooth temperature and conversion profiles, but complete curing occurs earlier in the third step of the cycle. For pipe walls thicker than 5.6 mm (base case), matrix curing is not completed under the imposed cycle. It is important to remark that an increase in the duration of the last step of the

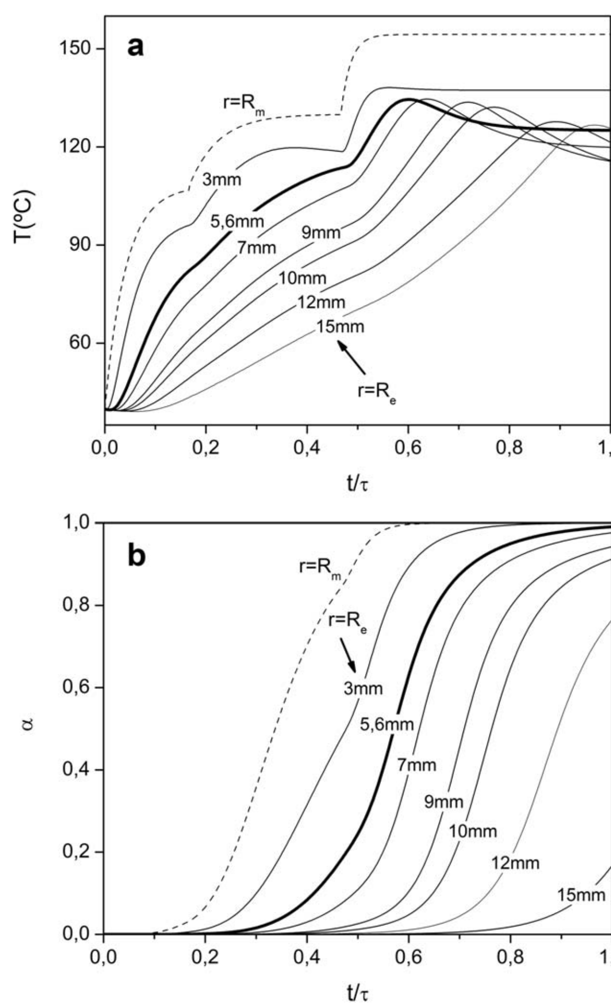

FIG. 8. Temporal evolution of temperature (a) and conversion (b) predicted at the inner and outer faces of pipes with various external diameters. Simulation conditions: case no. 5 (Table 2).

cycle to fulfill matrix conversion would lead to a broad radial conversion gradient within the pipe wall and therefore to low-quality pipes.

A different curing cycle should be designed for each specific pipe wall thickness.

CONCLUSIONS

A dynamic one-dimensional model is developed to simulate the internal heating curing process of GRE pipes produced by filament winding in a manufacturing plant located in Villa Mercedes, San Luis, Argentina. The model incorporates a mechanistic kinetic approach and it is calibrated and cross-validated using plant data.

The model comprises a useful tool that allows analyzing the impact of different processing variables on the internal heating curing process as well as designing proper curing cycles.

The main conclusions arisen from this work are:

– High-quality GRE pipes are produced if the matrix is gradually cured from the inside out with the development of smooth temporal and radial temperature profiles. Under this conditions: (i) the heat generated by the copolymerization reaction is efficiently transferred; (ii) at any time, the temperature decreases in the radial direction; (iii) uniform maximum curing rates are progressively achieved layer by layer.

– Ambient temperature strongly affects the curing process. There exists a critical temperature below which the curing cycle becomes inappropriate.

– An increase in the initial mandrel temperature does not shorten production time since it only affects the first step of curing where matrix conversion is negligible.

– The expected variability in fiber content does not practically influence the curing process. The curing cycle should be optimized for the lowest expected GF content.

– An increase in wall thickness necessarily implies a change in the curing cycle.

REFERENCES

1. H.C. Park, N.S. Goo, K.J. Min, and K.J. Yoon, *Compos. Struct.*, **62**, 51 (2003).
2. J. Zhang, Y. Xu, and P. Huang, *e-Polymer*, **10**, 41 (2013).
3. J.Z. Xu, M. Qiao, B. You, and Y. Yu, *J. Reinf. Plast. Compos.*, **31**, 605-620 (2012).
4. S.Y. Lee and G.S. Springer, *J. Compos. Mater.*, **24**, 1270 (1990).
5. E.P. Calius, S.Y. Lee, and G.S. Springer, *J. Compos. Mater.*, **24**, 1299 (1990).
6. S.Y. Lee and G.S. Springer, *J. Compos. Mater.*, **24**, 1344 (1990).
7. J.Z. Xu, B. You, and B.G. Wang, *Mater. Manuf. Process.*, **24**(**6**), 657 (2007).
8. D.H. Lee, S.K. Kim, W.I. Lee, S.K. Ha, and S.W. Tsai, *Compos. Part A: Appl. Sci. Manuf.*, **37**, 530 (2006).
9. T.A. Bogetti and J.W. Gillespie, *Cure simulation of thick thermosetting composites*. Technical Report BRL-TR-3121 (1991).
10. M. Li and C.L. Tucker III, *Polym. Compos.*, **23**, 739 (2002).
11. J. Xu, X. Wang, M. Qiao, and Y. Yu, *Polym. Polym. Compos.*, **19**, 319 (2011).
12. G. Ikonomopoulos and M. Marchetti, *Tech. Chron. Sci. J.*, **IV**(**1**), 67 (1998).
13. J. Zhang, Y.C. Xu, and P. Huang, *eXPRESS Polym. Lett.*, **3**, 534 (2009).
14. A.N. Mauri, N. Galego, C.C. Riccardi, and R.J.J. Williams, *Macromolecules*, **30**, 1616 (1997).
15. A.N. Mauri and C.C. Riccardi, *J. Appl. Polym. Sci.*, **85**, 2342 (2002).
16. H.A. Flores, L.A. Fasce, and C.C. Riccardi, *Thermochim. Acta*, **573**, 1 (2013).
17. API SPEC 15HR (R2010), *Specification for High Pressure Fiberglass Line Pipe*, American Petroleum Institute.
18. D. Santiago, G. Lombera, S. Urquiza, and S.M. Moschiar, *Mater. Res.*, **6**, 583 (2003).
19. B. Chern, T.J. Moon, J.R. Howell, and W. Tan, *J. Compos. Mater.*, **36** 2061 (2002).
20. B.A. Finlayson, *Nonlinear Analysis in Chemical Engineering*, Seatle (1980) 24-219
21. H.A. Flores, *Uso de Reactivo Diluyente en la Fabricación de Caños de ERFV*. Doctoral Thesis, Universidad Nacional de Mar del Plata, Mar del Plata, Argentina (2012).